# A VERY LONG-TERM MODEL OF THE CITY

Francisco Martínez-Concha, Universidad de Chile, Institute of Complex Engineering Systems (ISCI) – fmartine@ing.uchile.cl
Pedro Donoso, Universidad de Chile – pedrodonosos@gmail.com
Ricardo de la Paz-Guala, Universidad de Chile – ricardo.delapaz@uchile.cl
Daniel Martínez, Universidad de Chile – daniel.martinez.q@ug.uchile.cl
Leonel Gutiérrez, Universidad de Chile – lgutierreza@ing.uchile.cl

*Palabras clave: Urban evolution, Land use, Transport, Urban models, Cities' scaling*

## ABSTRACT

The very long-term evolution of cities' land use and transport (VLT-LUT) is modelled by developing a software simulating the effects of agglomeration economies, transport planning and urban sprawl. The cities' complexity is modeled in a market dynamic equilibrium framework. Our testing example simulates an artificial city for a scenario of a given road network and the agents' perception of agglomeration economies and increasing population from 1 to 30 millions inhabitants (around 300 years). Our results show the evolution of land-use by different residential and non-residential agents, the city size, land rents and travel times. They also show the super-linear increase in rents with population, in line with previous empirical and theoretical research, but the strength is differentiated by agents' behavioral scenario.

## 1. INTRODUCTION

In recent decades, complex models of cities have been formulated and applied worldwide, especially for urban policies analysis, generically named *land use and transport* (*LUT*) models or LUTE when it includes the production and labor markets (reviewed in Pagliara et al. (2010)). Such models share the approach of the interaction between land use and transport models with the aim to simulate city functions, usually in a time span of 20 to 30 years, through the interaction between representative household and firm agents and the movement of goods, providing different performance indices that allow the assessment of policy scenarios.

This medium-term utilitarian perspective is useful for planning, but lacks an understanding of the very long-term evolution of urban systems. In this wider perspective, there is evidence of a universal scaling law that emerges from worldwide urban big-data G. B. West (1999); G. B. West et al. (1999); G. West et al. (2001), similar to those observed in nature's complex systems G. West (2017). This scaling effect has profound implications in our knowledge of the evolution of urban

systems, because they are super-linear: output per capita increases with population, i.e., despite differences in history (cultural or geographical). G. West (2017) claims that cities follow a universal power law with a common scale parameter bounded to +/- 1.15. In contrast to this evidence, super-linearity is not a feature evident in current LUT models, as they are designed as sets of micro-economic rules econometrically adjusted to each context. To explain the scaling law, a theoretical land use-transport-economic activity integrated model (LUTE) was formulated Martínez (2016), then extended to interurban interaction in CLUTE Martinez (2018) through demographic migration (geographically and socio-economically). CLUTE provides a theoretical explanation of how the scaling factor emerges from the complex interaction between agents -households and firms- under stochastic behavior and land auctions in urban systems Martinez (2018).

Motivated by this constant evolutionary feature of cities, this research aims at reproducing it in a simulation platform. This paper reports -to our knowledge- the first attempt to simulate the evolution of cities in the very long term: a time period of about 300 years or from 1 to 29 million inhabitants. It is designed as a research platform to analyze different paths that a city may take in the very long-term according to its agglomeration economies and transport network, to extract lessons regarding the quality of life, productivity, and sustainability of the environment. As a proof of concept, here we report a prototype model, the *very long-term land use and transport* (*VLT-LUT*) software, where the simulated city is artificial, assumed isolated from other cities and detailed economic interactions are represented by accessibility indices obtained from the transport model.

We report preliminary results of the evolution of the fictitious city, simulated in a symmetric, flat and homogenous plain, initialized with population and firms distributed homogeneously in the space. Although it runs stepwise for exogenous increments of population (also representing time steps), the system dynamics is modeled keeping memory of the built infrastructure, allocation of agents and city size, thus making model steps interdependent.

The aim of this paper, at this stage of our research, is not to replicate the evolution of a real city, but to evaluate the performance of the VLT-LUT model under controlled scenarios. For example, given the complexity of the urban system, we analyze whether under symmetric conditions of the geography and the transport network, the form of the city remains symmetric in the very long-term, and whether the scaling law is replicated. The reported results show a symmetric evolution and we remark that the parameters values used in the simulation have been conveniently chosen in order to observe the performance of the model while keeping the simplicity required for this analysis.

## 2. THE MODEL

In this section, we present the *very long-term land use and transport* (*VLT-LUT*) model, describing the mathematical formulation of its sub-models. The evolution of time is represented, indirectly, by an exogenous population growth. The city size is endogenously modeled, which is a novel feature in land use models. The land use is based on the set of decisions made by residential and non-residential agents, regarding their willingness to pay (or bid) in auctions of different real estate units. The model is formulated as a set of fixed-point problems representing the mathematical complexity of the interactions among agents.

Let us consider a city composed of $I$ zones with equal area $A_i$, $\forall i \in I$, a transport network with underlying graph $G = (N, A)$, where $N$ is the set of nodes and $A$ the set of arcs. There are $K_R$ residential agents and $K_{NR}$ non-residential agents, all bidding for $V$ types of real estate. [1]

### 2.1. Demography and firmography

We use official available econometric models regarding population and economic growth assumptions. At each simulation step, the demographic and firmographic models estimate the disaggregation of population $N$ into residential (households) and non-residential (firms) agents. The shares of residential groups change over time, as population from lower incomes moves to higher ones. Non-residential agents' growth follows an exogenous evolution of the economy and population.

### 2.2. The land use model: Cube-Land

The demand of each agent $h$ is modeled by her willingness to pay or bid for each location defined by the zone $i$ and tne real estate type $v$, assumed as a stochastic variable $\hat{B}_{hvi} = B_{hvi} + \xi$, where $B_{hvi}$ is the deterministic part and $\xi$ an iid Gumbel term. The deterministic part is defined by $B_{hvi} = b_h + b_{hvi} + b$, where: $b_h$ represents the reserve utility that adjusts to reach a market location equilibrium for each type of agent $h$ (see fixed-point FPP3); $b$ represents a constant that adjusts bid levels to absolute prices in the economy; $b_{hvi}$ is agents $h$'s value of attributes describing location $vi$.

The allocation of agents to real estate option is modelled by the bid-auction logit probability model Martinez (2018) denoted $P_{h|vi}$, given by

$$P_{h|vi} = \frac{H_h e^{\mu\left(b_h + b_{hvi}\left(P_{\cdot|\cdot i}, S_{\cdot i}\right)\right)}}{\sum_g H_g e^{\mu\left(b_g + b_{gvi}\left(P_{\cdot|\cdot i}, S_{\cdot i}\right)\right)}}, \tag{FPP1}$$

where $P_{h|vi}$ maximizes the stochastic bids simulating an auction, $H_h$ is the total of agents type $h$ and $S_{vi}$ is the supply of real estate type $v$ in zone $i$. An important feature is that the set of attributes in $b_{hvi}$ includes endogenous variables $(P_{\cdot|\cdot i}, S_{\cdot i})$ describing neighbors' quality and agglomeration economies, i.e., $b_{hvi}(P_{\cdot|\cdot i}, S_{\cdot i})$. This defines the fixed-point problem (FPP1) $P_{h|vi} = f(P_{\cdot|\cdot i})$.

Rents $r_{vi}$ result from the auction process as the expected maximum willingness to pay at each location, given by:

$$r_{vi} = \frac{1}{\mu} \ln \left( \sum_h H_h e^{\mu B_{hvi}} \right) \tag{1}$$

where $\mu$ is the Gumbel scale parameter.

[1] For simplicity, whenever a sub-index is used (unless specified differently), it is understood that the statement is valid for the whole set that contains that sub-index.

The model predicts the supply of real estate units at each zone $S_{vi}$ by a logit model distributing new real estate supply stock among zones and real estate types:

$$S_{vi} = S_{0vi}\left(1 - k_{vi}\right) + \left(S - S_0 - S_D\right)\frac{e^{\lambda \pi_{vi}(S_{.i})}}{\sum_{w,j} e^{\lambda \pi_{wj}(S_{.j})}}, \tag{FPP2}$$

The total supply $S$ is defined as equal to the total number of agents, i.e., supply equal demand or every agent is allocated, then: $S = \sum_{vi} S_{vi} = \sum_h H_h$, $S_0 = \sum_{vi} S_{0vi}$. The model assumes a demolition rate $k_{vi}$ of the supply at the previous simulation step $S_{0vi}$, then demolished real estate stock is $S_D = \sum_{vi} S_{0vi} k_{vi}$ and the new stock is $S - S_0 - S_D$. The developer's profits is assumed stochastic, defined as $\hat{\pi}_{vi} = r_{vi} - C_{vi} + \varepsilon$ with expected value $\pi_{vi}$, where $\varepsilon$ is a Gumbel term with scale parameter $\lambda$. Since rents depend on the supply portfolio, we observe that the supply model defines a fixed-point problem (FPP2) on supply $S_{vi} = f(S_{..})$.

The equilibrium between demand and supply is reached assuming that all agents are allocated, which is attained by adjusting the reservation bid $b_h$ variables by solving the demand-supply equation $H_h = \sum_{vi} S_{vi} P_{h|vi}(b_h)$, which is a fixed-point problem on $b_h$ for all $h$ (FPP3):

$$b_h = -\frac{1}{\mu} \ln\left(\sum_{vi} S_{vi} e^{\mu(b_{hvi} - r_{vi}(b_h))}\right) \tag{FPP3}$$

Cube-Land model solves FPP3 providing the location matrix $H_{hvi} = S_{vi} P_{h|vi}$ Martinez (2018).

The development cost $C_{vi}$ depends on land prices, $p_i$, an endogenous variable regarding the following recursive sequence: rents $r_{vi}$, which depend on supply $S_{vi}$, which depends on profit of real estate $v$, $\pi_{vi}$, which depend on building costs $C_{vi}(p_i)$, thus $p_i = f(p_i)$ is a fixed-point problem referred to as FPP4.

We consider densities and access indices as the endogenous location attributes in agents' willingness to pay assessment. Densities represent a location externality in the bid function $b_{hvi}$, i.e., socioeconomic quality of the neighborhood for residents and agglomeration economies for non-residents. Thus, agents' bids depend on the location matrix, i.e., on the location probabilities of all agents $b_{hvi}(P_{hvi})$. At each zone $i$, we define the density of each agent $h$ in zone $i$, as:

$$\rho_i^h = \sum_{v=1}^{V} H_{hvi} \frac{\theta_h}{A_i}, \tag{2}$$

where parameter $\theta_h$ is the average number of households' agents $h$. We also consider the aggregated densities of residential agents $\rho_i^{res}$ and of non-residential agents $\rho_i^{nores}$.

Access indices are also endogenous variables depending on densities and transport costs. For each zone $i$, access is described by two components, accessibility ($acc_i$) and attractiveness ($att_i$) of residents to non-residential activities, defined as follows:

$$acc_i = \ln\left(\sum_{j=1, j\neq i}^{I} \rho_j^{nores} e^{-\alpha_0 \tau_{ij}}\right), \tag{3}$$

$$att_i = \ln\left(\sum_{j=1,j\neq i}^{I} \rho_i^{res} e^{-\alpha_0 \tau_{ji}}\right), \tag{4}$$

where $\tau_{ij}$ represents the expected minimum travel time between the centroids of zones $i$ and $j$, and parameter $\alpha_0$ adjusts the perception sensitivity to travel costs.

### 2.3. The traffic model

We apply the Markovian traffic equilibrium (MTE) Baillon y Cominetti (2008), a private vehicles assignment model, where trips result from the recursive choice of the exit arc at each network node. At each node $n$ and for each destination node $d$, MTE assigns a probability $P_a^d$ of the aggregated flow -from all origins arriving at node $n$ going to destination $d$- $x_n^d$, that exits by each outgoing arc $a = (n, m) \in A_n^+$ (the set of arcs leaving node $n$). It applies a logit probability with scale parameter $\delta$, whose criterion is that travelers choose the arc with the expected minimum travel time between nodes $n$ to $d$ by using arc $a$, denoted as $z_{ad}$. Thus, we have that:

$$P_a^d = \frac{e^{-\delta z_{ad}}}{\sum_{b\in A_n^+} e^{-\delta z_{bd}}}. \tag{5}$$

where $z_{ad}$ is the sum of the travel time in arc $a$, $t_a$, plus the expected minimum time from node $m$ ($a$'s end node) to destination node $d$, $\tau_{md}$, thus $z_{ad} = t_a + \tau_{md}$. Note that expected minimum travel time depends on the remaining trip to the destinations, i.e., $z_{ad}\,(\tau_{..})$, then, the MTE model solves fixed-point problem FPP5 on $\tau_{md}$:

$$\tau_{md} = -\frac{1}{\delta}\ln\left(\sum_{a\in A_m^+} e^{-\delta z_{ad}(\tau_{..})}\right). \tag{FPP5}$$

### 2.4. Trip generation and distribution model

The land-use model output provides the allocation of agents in the city, which is used to estimate trips between zones using private transport costs provided by the traffic model. The trips generation model (GDT) estimates the number of daily trips per household type generated at each zone as a rate per household. The trip distribution model estimates the number of trips attracted by each zone as a linear function of the non-residential agents' density. Trips generated and attracted define the marginals of the trip matrix. The origin-destination matrix $V_{ij}$ is calculated by a standard doubly constrained entropy model, which solves a fixed-point problem (referred to as FPP6) to estimate the Lagrange multipliers of the marginals, as in Macgill (1977). This model uses travel times between zones provided by the traffic model (Subsection 2.3).

### 2.5. Urban spatial border

As population grows, the city sprawls and its border has to be modeled. We assume that urban (residential and non-residential) and rural agents compete for locations in a city border model. For each zone land, suppliers bid according to their the maximum expected profit $\pi_i = \max_v (r_{vi} - C_{vi})$, while rural agents bid an exogenous agricultural rent value $R_A$. If suppliers' bid is less than $R_A$, then the zone remains agricultural and it is considered out of the urban boundaries; otherwise, it is included in the set of urban zones; once a zone becomes urban it remains urban forever. Regarding the whole city sprawl, we name it *expanding city* when there are rural zones in the modeling spatial grid, otherwise, we call it a *saturated city* where no expansion is possible, i.e., once a city becomes a saturated remains as such for ever. This allows the city to extend its urban limits according to the growing population, following Alonso (1964)'s rule to define the city boundary as an auction between rural and urban land use.

## 3. THE DYNAMIC NATURE OF THE VLT-LUT MODEL

At each population step the land use model attains a market equilibrium between demand and supply, however, the conditions of such equilibria depend on the status of the city in the previous step, which induces a dynamic process. Since equilibrium is unique Martinez (2018), the set of mutually dependent equilibrium sequences is unique, although it depends on the initial conditions in step 1. This theoretical argument is analyzed in our case study.

The temporal dependency has two reasons:

- The demolition of infrastructure (see FPP2) keeps memory of the previously built stock of real estate, allowing only a proportion to be renewed.
- The urban border evolution keeps memory of the zones previously belonging to the city.

Both features define the conditions for the equilibrium at each population step, thus rent, land-use and densities acquire a dynamic nature. From this, the accessibility and attractiveness of each zone, and thus the associated trips and travel times have a dynamic dependence.

## 4. SOLUTION ALGORITHM

We propose a solution algorithm over a discrete set of population steps representing time denoted $N_0, ..., N_F$. The routine can be summarized as follows:

- **Initialization Iteration 0:** An initial population level $N_0$ is set and distributed by agent socioeconomic types using the demographic model and the number of non-residential agents

is estimated using the firmography model. An exogenous distribution of agents is allocated among zones, which allows to compute initial values for the variables using free-flow travel times. The urban limit is set as an initial parameter, and accessibilities and attractiveness are computed according to Equations 3 and 4. These initial conditions applied to the LUT model define the initial real estate supply.

- **Iterative process: LUT for $N_1, ..., N_F$:** At each iteration $i$, the algorithm performs the LUT model depicted in Figure 1 for the population step $N_i$, obtaining the output solutions. Given that the model holds memory of past buildings, the resulting supplies $S_{vi}$ are used as inputs for the following iteration $N_{i+1}$.

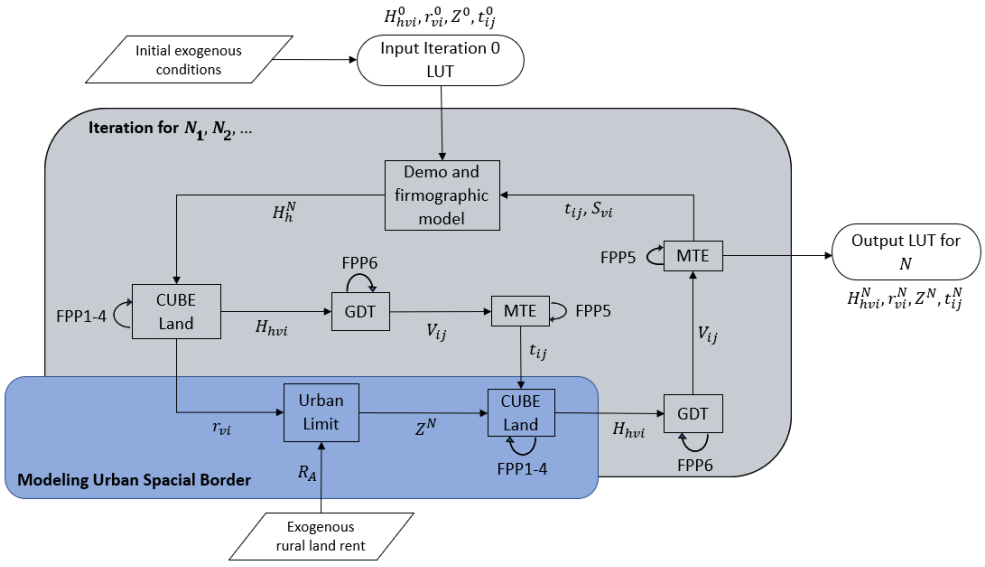


Figura 1: General algorithm scheme.

Following Figure 1 we describe the algorithm. The demography and firmography models yield $H^N_h$ agents per type, which inputs the Cube-Land model, along with the variables from the previous step: supply, densities, accessibility and attractiveness attributes and city border. This model solves fixed-point problems FPP1 to FPP3 yielding updated LU equilibrium variables: allocation $H_{hvi}$, supply $S_{vi}$ and rents $r_{vi}$. Then, the set of land prices $p_i$ are computed to calculate building costs $C_{vi}$, which are used to update suppliers' profits and iterate with Cube-Land simulating fixed-point problem FPP4 until a convergence criterion is attained.

Next, the algorithm branches into two processes: definition of the urban border and simulation of the transport system. The calculation of the updated urban limit is performed by the land auction process, given agricultural land rent $R_A$, and new zones may be added to the set of urban zones $Z^N$. The second branch calculates the number of daily trips between zones $V_{vij}$ solving the fixed-point FPP6 for a given network. Then, the traffic model assigns these trips to different routes in the network where vehicles' congestion requires solving an equilibrium, which defines fixed-point problem FPP5. The output yields travel times on arcs and routes, and the expected minimum time between zones $t_{ij}$, which allows updating accessibility and attractiveness attributes.

Then, the algorithm runs Cube-Land with updated access indices and city border, followed by the transport model to obtain the estimate of the land-use and transport profile for population step $N$.

## 5. SIMULATION

As a proof of concept, we present the outputs of a computational implementation of the algorithm applied to an artificial city. Before going further into the description of the studied scenario and, later, the results, it is important to highlight the complexity of the simulation process of a city.

Even though we present results on an artificial city with conveniently chosen parameters and data, the process of building this proof of concept is far from unrealistic. As established in Section 2 by the model specification, and then in Section 4 by the algorithm, several equilibrium and subroutines are embedding a proper algorithm.

Since we simulate an artificial city, the model parameters were chosen carefully. For example, if the referential agricultural rent is too low, the city sprawls quickly, densities are low (as population grows linearly), and we lose the effect of high accessibilities and attractiveness that occur when the city is compact in its early stages. On the other hand, if the referential agricultural rent is too high, the city may even not sprawl at all, resulting in high densities in a compact city while multiple rural zones are still available.

### 5.1. Simulation scenario

The city is spatially defined in a featureless squared plain with 100 km per side, divided into a squared grid of 400 equal size zones of 25 $km^2$, denoted $i$, $i = 1, ..., 400$. The road network is a grid of secondary roads of one lane per direction plus a cross shape of highways with two lanes per direction (see Figure 3).

The time horizon is approximately 300 years, represented through population steps from $N = 1$ to $N = 29$ million inhabitants, with increments of 2 million inhabitants. There are 5 types of agents, $h = 1, 2, 3$ being residential and $4, 5$ non-residential, and 5 types of real estate (Tables 1 and 2).

| $h$ | characteristic | label |
|---|---|---|
| 1 | low-income home | residential |
| 2 | mid-income home | residential |
| 3 | high-income home | residential |
| 4 | industry | non-residential |
| 5 | commerce | non-residential |

Tabla 1: Types of agents.

The following attributes describe agents and real estates categories:

| $v$ | characteristic |
|---|---|
| 1 | small house |
| 2 | big house with yard |
| 3 | appartment/office |
| 4 | commercial store |
| 5 | large land lot |

Tabla 2: Types of real estate types.

- Residents are categorized by income $I_h$, which is equal within the group and exogenous, with $I_1 = 13{,}3[UF]$, $I_2 = 25{,}6[UF]$, and $I_3 = 38{,}0[UF]$ (UF is a Chilean currency).
- At the initialization step, the demographic and firmographic models split the initial population among the five types of residents according to the initial values. Then, the share of each population category remains constant along the simulation.
- Real estate types $v = 1, .., 5$ are characterized by two attributes: the floor space or building size $BS_v$ and land lot size $LS_v$, whose values are shown in Table 3.

| $v$ | 1 | 2 | 3 | 4 | 5 |
|---|---|---|---|---|---|
| $BS_v$ | 35 | 70 | 50 | 50 | 300 |
| $LS_v$ | 35 | 140 | 1 | 50 | 500 |

Tabla 3: Attributes of real estate types $v$ $[m^2]$.

Land prices are calculated from rents as follows:

$$p_i = \min_w \frac{r_{wi}}{LS_w}. \tag{6}$$

The cost of real estate $v$ in zone $i$, $C_{vi}$, is the construction cost plus the land lot costs, thus, we have that $C_{vi} = \alpha BS_v + p_i LS_v$, where $\alpha$= 0.009 $[UF/m^2]$.

We define the bid of a resident agent $h = 1, 2, 3$ for a real estate $vi$, as:

$$b_{hvi} = \alpha_h I_h + \alpha_{1h} acc_i + \alpha_{2h} \rho_i^{res} + \alpha_{3h} BS_v + \alpha_{4h} LS_v, \tag{7}$$

the bid of industrial agent $h = 4$, as:

$$b_{4vi} = \alpha_{1h} att_i + \alpha_{2h} \rho_i^{ind} + \alpha_{3h} BS_v + \alpha_{4h} LS_v, \tag{8}$$

and the bid of commercial agent $h = 5$, as:

$$b_{5vi} = \alpha_{1h} att_i + \alpha_{2h} \rho_i^{com} + \alpha_{3h} BS_v + \alpha_{4h} LS_v. \tag{9}$$

where values of $\alpha$ parameters are chosen from experts' experience and shown in Table 4. The specification of bid functions highly influences the simulation results of the spatial allocation patterns analyzed below. Notice that, for simplicity, bid functions are linear, without saturation effects.

Another feature is that agents perceive zonal -or neighbor- attraction but only to their own group density, i.e., self-attraction, without cross attraction between agent groups. Complementarily, cross attraction between agents across zones occurs in access measures ($acc$ and $att$). Additionally, the transportation system influences bids through access measures. Supply and demand logit probabilities have scale parameters, $\lambda$ and $\mu$ respectively, both equal to 0.03.

| $h$ | $\alpha_h$ | $\alpha_{1h}$ | $\alpha_{2h}$ | $\alpha_{3h}$ | $\alpha_{4h}$ |
|---|---|---|---|---|---|
| 1 | 0.10 | 6.00 | 0.0030 | 0.002 | 0.002 |
| 2 | 0.15 | 6.75 | 0.0010 | 0.003 | 0.003 |
| 3 | 0.20 | 8.25 | 0.0005 | 0.004 | 0.004 |
| 4 | - | 6.00 | 0.0100 | 0.010 | 0.050 |
| 5 | - | 8.25 | 0.0020 | 0.050 | 0.010 |

Tabla 4: Bid functions parameters.

The transport model considers the grid depicted in Figure 2, with 400 zones and a symmetric transport network (1 lane per direction roads) with a central cross-shaped highway (2 lanes per direction). As shown in Figure 2, at each zone we define road 16 nodes, a fictitious centroid node (where trips are generated and end) and 28 bidirectional arcs (4 imaginary connecting the centroid..

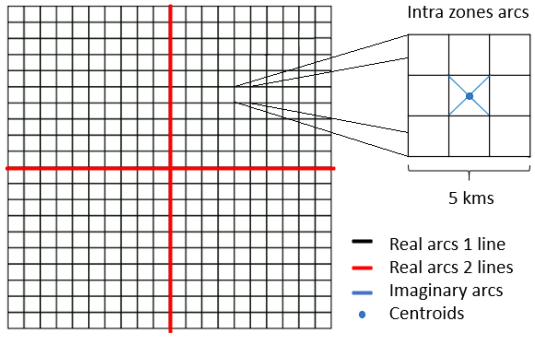


Figura 2: Structure of the network grid and zones.

The travel time of arc $a$ ($t_a$) depends congestion, i.e., on its flow $w_a$ (Equation 10),

$$t_a = \begin{cases} t_a^0 \left(1 + b_a \left(\frac{w_a}{c_a}\right)^{p_a}\right), & \text{if } w_a \leq c_a \\ 30 \text{ [min]}, & \text{otherwise}, \end{cases} \tag{10}$$

where: $t_a^0$ is the free-flow travel time; $c_a$ is the arc capacity; $b_a$ is a congestion parameter (Table 5) and $p_a = 3$ is a fixed parameter. Variable $w_a$ aggregates the flows of arc $a$ going to each destination $d$, denoted as $v_a^d$ and computed as $v_a^d = x_i^d P_a^d$, i.e., $w_a = \sum_d v_a^d$. This assumes that congestion increases up to a maximum arc time of 30 minutes, a fictitious limit to control numeric issues. These features remain constant along the simulation, the only exogenous variable is population.

| type of arc $a$ | $t_a^0\ [min]$ | $b_a\ [\,]$ | $c_a\ [veh/h]$ |
|---|---|---|---|
| imaginary | 0.1 | 0 | 1 |
| real: bidirectional-1 lane | 3.0 | 9 | 40000 |
| real: bidirectional-2 lanes | 2.0 | 14 | 120000 |

Tabla 5: Values for the congestion function parameters for every type of arc.

## 5.2. Urban sprawl

The evolution of cities is geographically perceived by urban sprawl. Figure 3 depicts the number of urban zones at each population level. Note that the curve's increases monotonically because once a rural zone becomes urban, it remains urban even if land rent becomes lower than the threshold given by the referential agricultural rent. The city shows three sprawl phases. Initially, up to 3 million inhabitants, the city border remains unchanged, keeping the size of the initial setting. Then, up to 23 million, despite population increasing linearly, the city sprawls with a non-linear shape; this effect might be caused by the fixed transportation network. At 23 million inhabitants the city reaches the limit of the grid, i.e., 400 zones, simulating a geographical or regulatory limit. An interesting evolution point occurs around 11 million inhabitants, where the city starts an accelerated urban sprawl, which we discuss below.

An important observation is that sprawl is symmetrical, following the layout of the symmetric transportation network. This feature is relevant because it is not for granted in a complex non-linear model, where the land use equilibrium is mathematically solved from a set of fixed-point problems, combining multiple agents' behavior and real estate supply options, and, moreover, interacts with an also complex transportation network equilibrium.

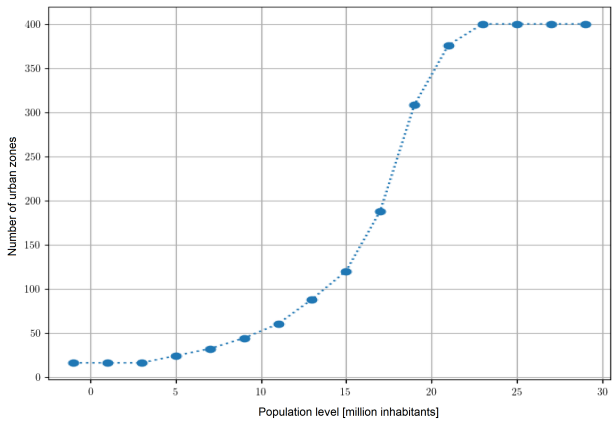


Figura 3: Evolution of number of urban zones.

Figure 4 depicts the sprawl evolution from a bird-eye view, showing that the urban border expands from the center to the outskirts of the city. Initially with a diamond shape caused by the cross-shaped highways network. The accessibility effect of highways diminishes in a large city (after 11 million onwards).

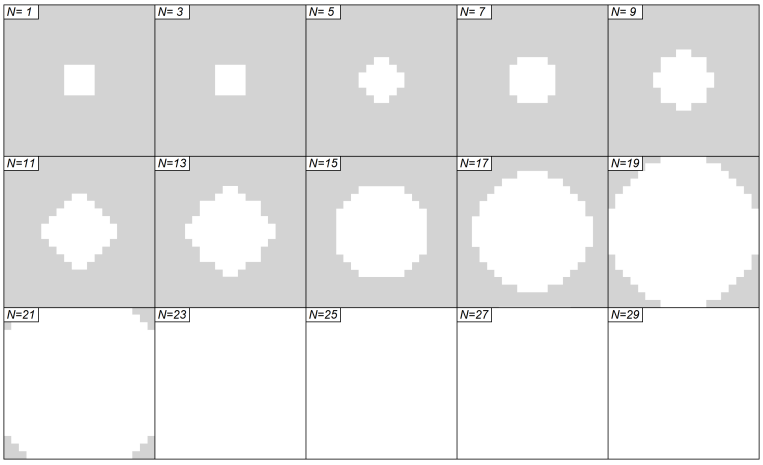


Figura 4: Evolution of urban limit. Urban zones in white, rural zones in grey.

### 5.3. Densities

Figure 5 shows the evolution of the urban zones average densities for each agent type: residential, industrial and commercial. Considering the evolution of the urban sprawl, note that initially, when sprawl is null or at low pace (up to 11 million), average densities increase, followed by a fast sprawl where densities fall up to a stable situation. Maximum densities follow a similar tendency, except for the industrial case that increases fast after 20 million inhabitants. This illustrates that the pressure of the increasing population densities pushes the city to sprawl, but only after population increases enough to push bids up to outbid the rent in rural land (see the section rents below).

The evolution of the population's location is specific for each agent type, as shown in Figure 6 for residential, industrial and commercial, whose patterns are dependent on the bid functions specified in Equations 7, 8 and 9.

Observe that for a small city, up to 7 million, commercial activities dominate the city center, while residents locate in a ring around the center and industry moves out far from the center. Then, during the city sprawl process (up to 21 million), commerce continues to dominate the center, but it also concentrates in a ring and in hotspots with higher agglomeration. Residents locate in two rings, one around the city center and another beyond the commerce ring, i.e., filling the space left empty by commerce. Commerce and residents' rings extend along the highway's axes. Industry moves to the edge of the city following the city sprawl. When sprawl slows down (after 21 million) a more complex pattern of residential and commercial agglomeration emerges, with up three rings of commerce and residents interspersed, with a commercial city center.

This commerce-residents rings pattern has an explanation in the mutual dependency between commerce and residents on accessibility and attractiveness (see Equations 3 and 4), which are represented in bid functions. The transportation network effect is evident in the extension of commerce and residents' rings along highway axes.

We have analyzed spatial densities aggregating the residential agents, while Figures 7 and 8 di-

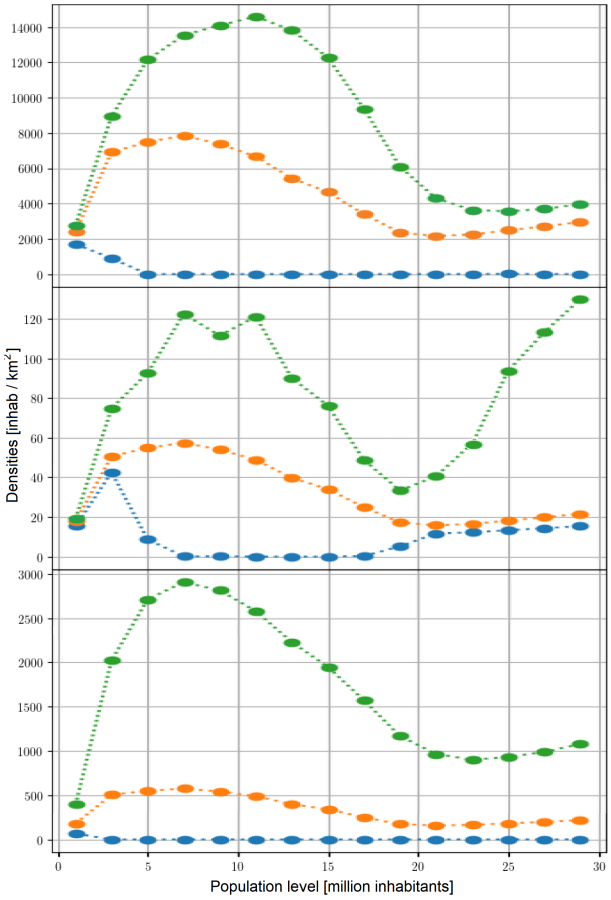


Figura 5: Evolution of densities: minimum (blue), average (orange), and maximum (green). For aggregated residential agents (top), industrial agents (center), and commercial agents (bottom).

saggregate average zonal densities of residential agents into their respective income groups: low income ($h = 1$), mid income ($h = 2$), and high income ($h = 3$), although this patterns depends on the specific bid functions considering self-group attraction (Equations 7, 8 and 9). Figure 7 shows a similar evolution of agglomeration, or segregation by income group, they initially agglomerates (high maximum density) but then, as the city sprawls, they disperse in the city; an exception is the high income group that over 21 million inhabitants the maximum density increases steeply.

In Figure 8 we observe spatial segregation. The dominant pattern is: the poor group locates in an inner ring around the commercial center, the middle income in a second ring and the rich in the third outer ring. When sprawl stops at 21 million inhabitants, the inner and second residential rings mix with commerce. These results show an interesting and differentiated evolution of the spatial allocation of agents' groups, showing segregation between socioeconomic groups as an expected outcome of bids specified, on purpose, with self-attraction. Cross attraction may be a realistic model in some real situations, but we aimed at detecting dynamic patterns in the simplest case.

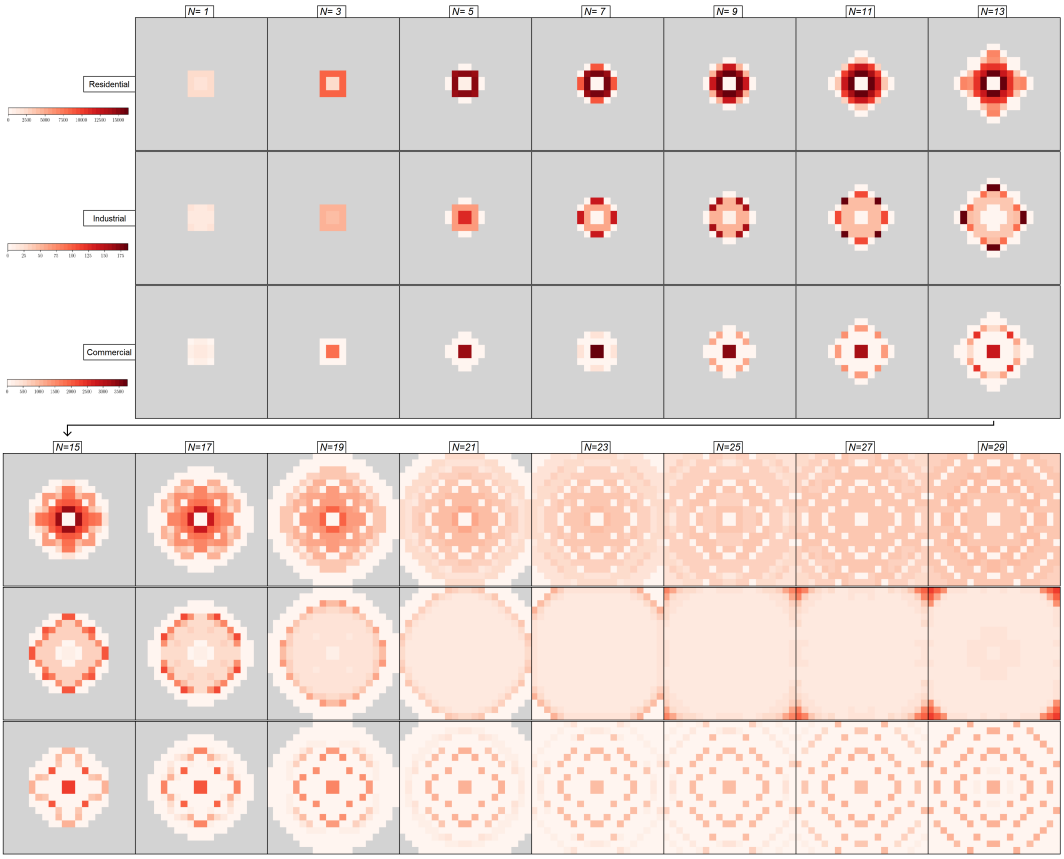


Figura 6: Spatial evolution of densities. Residential (top), industrial (center) and commercial agents (bottom).

### 5.4. Real estate stock

The real estate supply of each type $v = 1, ..., 5$, shown in Figure 9, depicts a very similar evolution across real estate types. They peak after the rapid sprawl of the city, at 13 million inhabitants, a delayed reaction associated with the limited rate of demolition. This figure describes an overall pattern: once the city expands geographically, the built stock density is very similar across the city (minimum similar to maximum values).

### 5.5. Rents

The evolution of zone average real estate rents of urban zones is shown in Figure 10. It shows a maximum peak delay with respect to the urban sprawl. Mean values of rents are very stable along the simulation period although gradually increasing. Figure 11 shows the spatial pattern of real estate rents, where maximum values are located in the inner ring around the city center, notably not in the center. After the city reaches the grid limits (400 urban zones at 21 million) the maximum values pattern evolves, forming a second ring, which follows residents' locations.

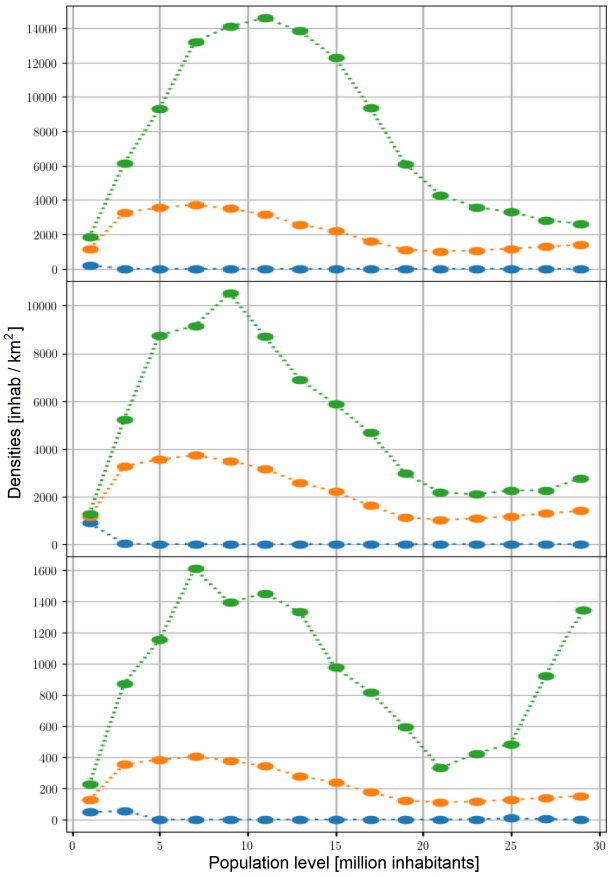


Figura 7: Evolution of residents agglomeration by income group. Minimum (blue), average (orange) and maximum (green) zonal densities of agents: low income (top), middle income (center) and high income (bottom).

We now analyze the evidence of a scaling law between the simulated rents and the population in our artificial city. The power law of the city's aggregated rents $R$ on the population $N$ is $R = \beta_0 N^{\beta_1}$, where the theory Martinez (2018) justifies $1 \leq \beta_1 < 2$ and, based on empirical evidence in G. West (2017) it is considered that $1 \leq \beta_1 \leq 1{,}15$ is expected. The estimated parameters are $\hat{\beta}_0 = 16{,}3$ and $\hat{\beta}_1 = 1{,}048$, with a regression fit index $R^2 = 0{,}9998$, meaning that the power law model explains almost 100 % of the whole variability of the data obtained from the simulation. Our results support the empirical evidence and the theory of a super-linear scaling of rents, however the scaling parameter $\hat{\beta}_1$ is lower than the estimated using data in many cities G. West (2017). However, we observe that our simulation assumes that residents' income is fixed over time, which is against the empirical and theoretical studies mentioned above where wages scale non-linearly; this assumption reduces the scaling effect of bids and rents. Additionally, we remark that this outcome is obtained in a city free to sprawl, i.e., no urban regulations affects land prices, then the scaling rents is essentally the direct effect of an increasing economic interaction between agents with population.

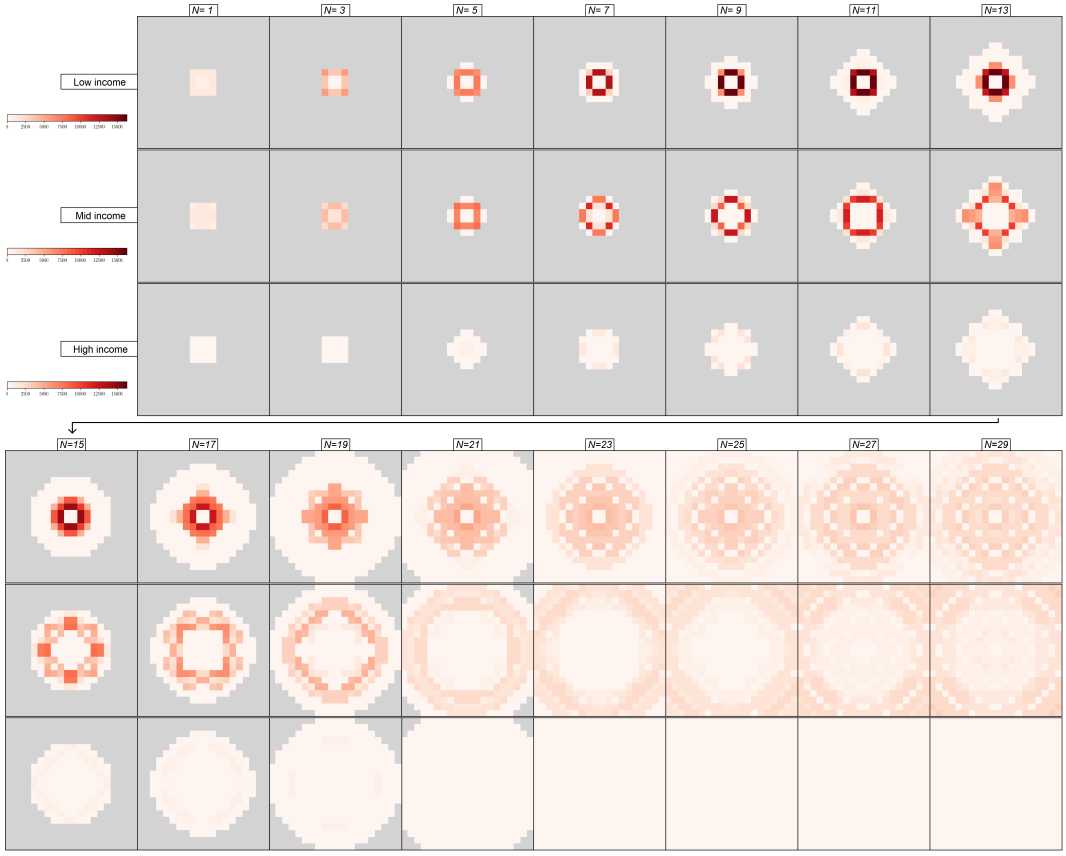


Figura 8: Evolution of spatial densities residential agents: low income (top), mid income (center), and high income (bottom).

### 5.6. Accessibility

Accessibility and attractiveness are calculated for all zones, independently on whether they are urban or rural. Figures 13 and 14 show the local evolution of these zonal variables. Initially accessibility increases monotonically to the center of the city (up to 11 million), then a ring appears followed by cross-shaped hotspots (at 21 million), when accessibility becomes more evenly distributed. Attractiveness is also monotonically increasing to the center, with a center radio that increases over time up to cover the whole city (25 million) when this index is very homogeneous.

### 5.7. Transport

Travel times between zones are the most representative of the transport variables, as they define the trip costs perception of the users. We present two types of travel times, the trip average time that takes to travel from the origin and the destination of all OD pairs, shown in Figure 15, and the average travel time in arcs, shown in Figure 16.

Trip travel times gradually increase over time, particularly maximum values. The intuition that

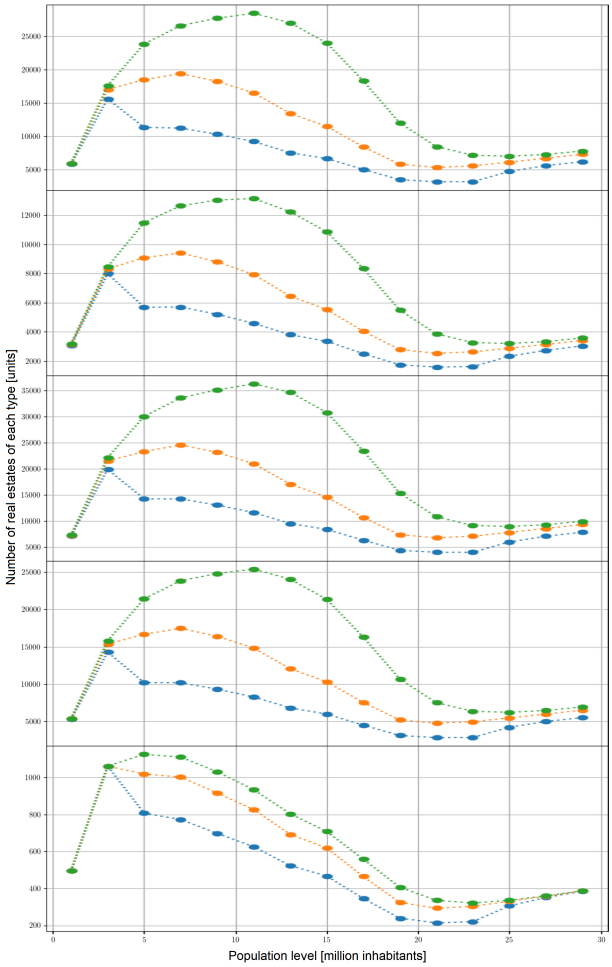


Figura 9: Number of real estate units by zone: minimum (blue), average (orange), and maximum (green) zonal supplies of real estate $v = 1, ..., 5$ (from the upper plot and below, respectively).

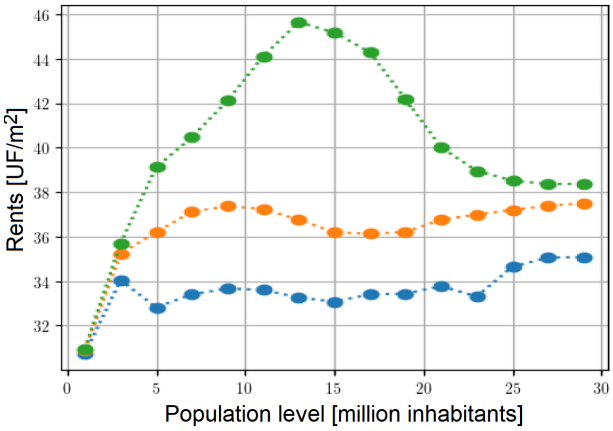


Figura 10: Weighted average rents according to real estate supply. Minimum (blue), average (orange), and maximum (green)

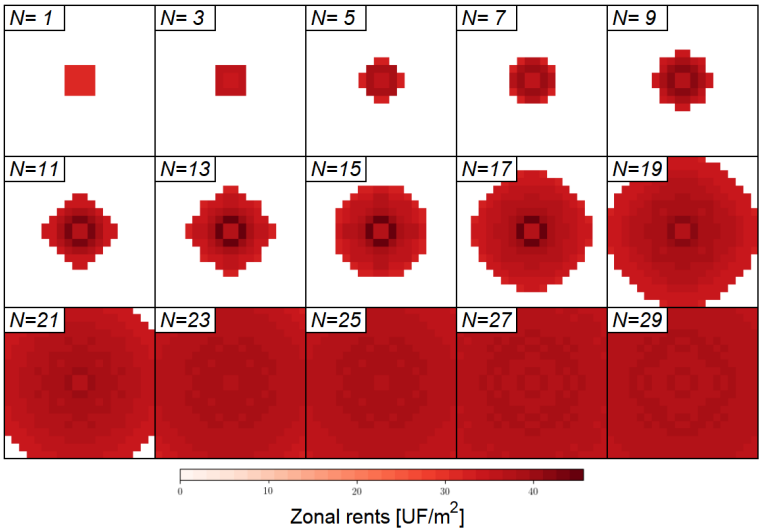


Figura 11: Weighted zonal rents according to real estate supply.

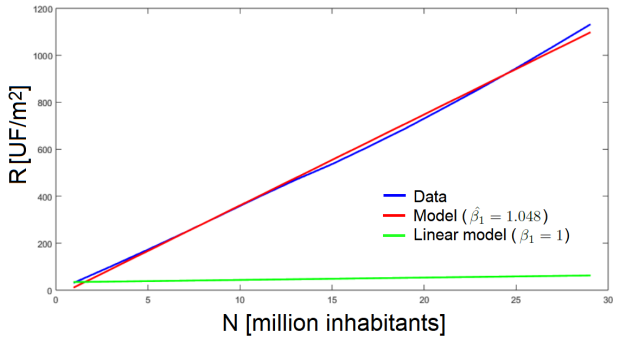


Figura 12: The power law between total rents and population

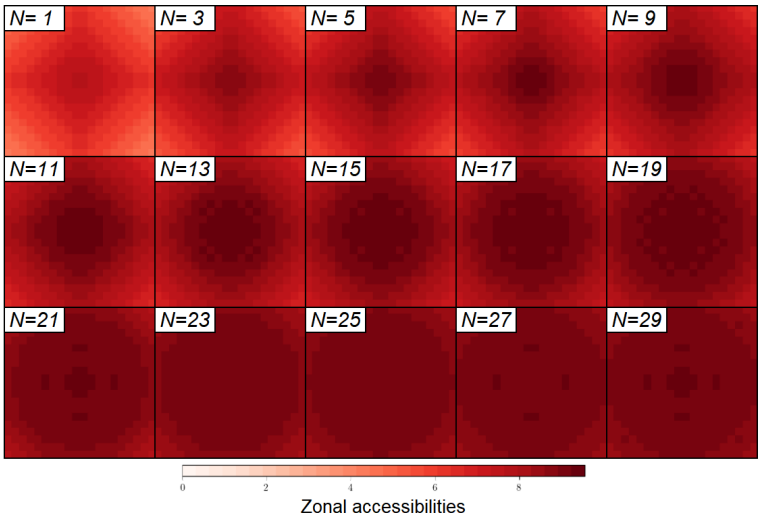


Figura 13: Zonal accessibilities.

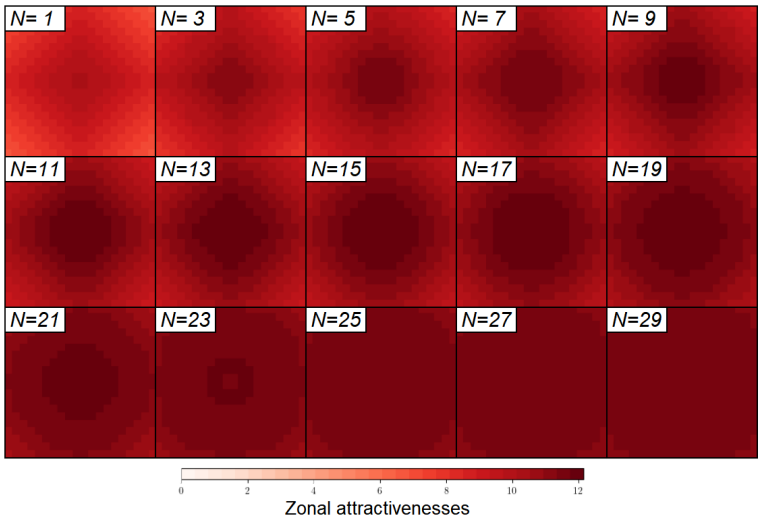


Figura 14: Zonal attractiveness.

larger cities induce longer travel times is confirmed to some extent, but the pace is much lower than the city expansion. This is the consequence of the relocation of residential and non-residential activities over time, in a way that trips that initially concentrate their destinations in the city center, then redirect to the first and second rings of commercial activities.

The average travel times travel in arcs show a steep peak in maximum values, followed by a fall when the city sprawls. Therefore, sprawl induces a significant reduction in traffic congestion. Notice also, that the peak time is lower than the 30 min limit imposed in Equation 10 avoiding unrealistic time estimates.

In sum, in larger cities, activities are allocated to minimize travel time and, in that way, compensate for larger distances and control excessive congestion.

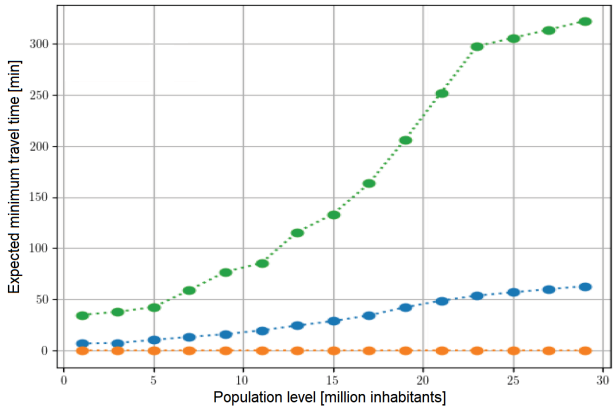


Figura 15: Trip travel times: minimum (blue), average (orange) and maximum (green), of the average expected travel times between the origin and destination zones.

Other relevant transport variables are the flows of trips in the network, where we have assumed

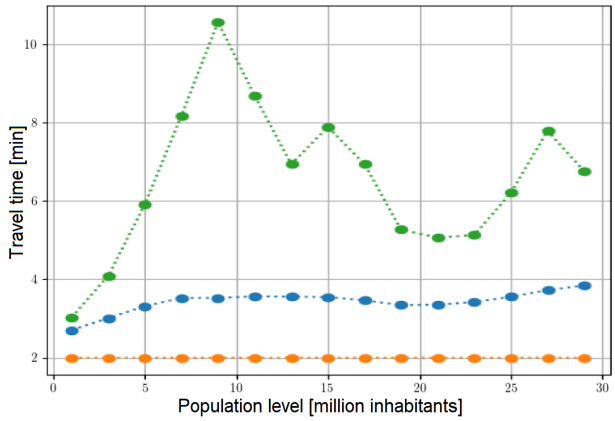


Figura 16: Arc travel times: minimum (blue), average (orange), and maximum (green).

one flow unit (vehicle) per traveler and private transport only. Again, we consider the evolution of average trip flows generated for each OD pair and the average flow assigned to each arc. Figure 17 shows a similar peak than previous figures, followed by a decline in maximum flows. This means that, as city sprawls, the trip destination patterns show a distribution in the city in a larger set of destinations. At the microscopic level of arc flows, Figure 18 shows that this variable initially increases steeply and then remains with high maximum flows.

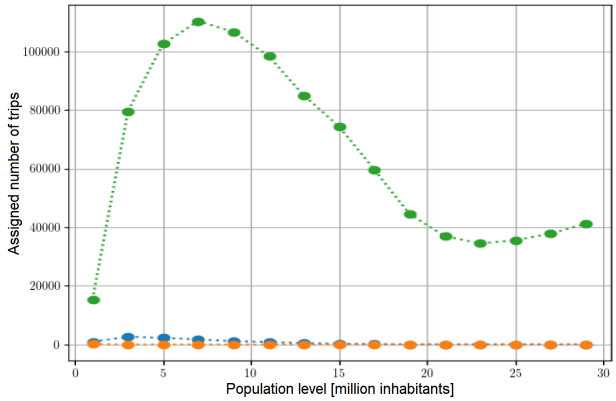


Figura 17: OD trip flows. Minimum (blue), average (orange, over blue), and maximum (green).

## 6. FINAL REMARKS

The analysis shows that the city evolves symmetrically, despite the system's mathematical complexity. Nevertheless, we report that the system is sensitive to very small asymmetrical values (of the order of $10^{-10}$) in the MTE model estimations of travel time. The observed symmetry is obtained when the equilibrium convergence criterion is set for physically meaningful values of trips, i.e., vehicles per hour, otherwise, an initial small asymmetry grows with population inducing asymmetric location patterns. Of course, symmetry is not a realistic feature of real cities, but it is a necessary property of the model under the fictitious symmetric conditions set in our simulation scenario.

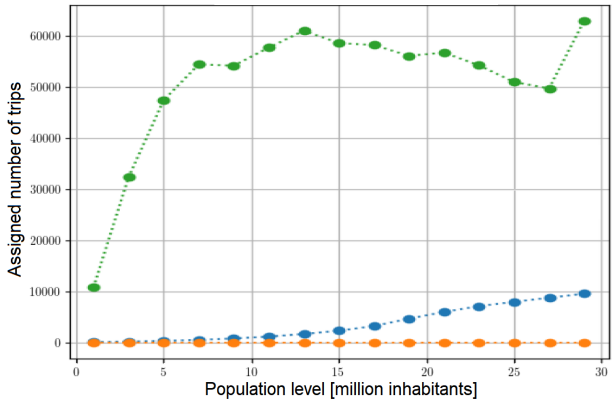


Figura 18: Arc flows. Minimum (blue), average (orange), and maximum (green).

Another observation of the model performance is non-fulfillment of space, i.e., space land in urban zones if not fully developed into real estate, while the city sprawls. This is a feasible outcome in this land-use model, because no equation imposes land fulfillment and its level is the result of the economic equilibrium. Future research may analyze the role of urbanization costs in zones integrated to the urban area, which has not been included in our simulation.

It is important to highlight that this model is dynamic, not just a successive simulation of a static city with different population levels. Its dynamics depends on several memory features: the city size at each population level depends on past urban borders, the real estate stock depends on previous development and partial building demolition, and agglomeration patterns of specific agents affect the next simulation steps.

We conclude that socioeconomic segregation and commercial agglomeration economies emerge as a result of the agents' behavior represented in bid functions. The specific segregation pattern depends on the parameters' set chosen for our simulation, then a complete analysis of segregation outcomes from different bid functions is also a topic for future research.

Another important conclusion is that the transport network shapes the city's form. In the performed simulations, we let the transport network be highly simplified (private transport and a network with only a cross-shape highways) to emphasize how transport capacity induces location patterns. Thus, the urban form evolved from a small monocentric city to a shape that extends along the highways' cross.

The emerging lesson is that roads infrastructure significantly shapes cities, while agglomeration economies are endogenous effects resulting from agents' behavior.

This model bring a new opportunity to investigate numerous research topics, e.g., policies on zoning, subsidies and transport networks, to obtain lessons about their long-term impacts and to analyze how the scaling law of rents is affected by them.

## REFERENCIAS

Alonso, W. (1964). **Location and land use: toward a general theory of land rent**. Harvard university press.

Baillon, J.-B., y Cominetti, R. (2008). Markovian traffic equilibrium. **Mathematical Programming**, 111 (1-2), 33–56.

Macgill, S. M. (1977). Theoretical properties of biproportional matrix adjustments. **Environment and Planning A**, 9 (6), 687–701.

Martinez, F. (2018). **Microeconomic modeling in urban science**. Academic Press.

Martínez, F. (2016). Cities' power laws: the stochastic scaling factor. **Environment and Planning B: Planning and Design**, 43 (2), 257-275. Descargado de https://doi.org/10.1177/0265813515604245 doi: 10.1177/0265813515604245

Pagliara, F., Preston, J., y Simmonds, D. (2010). **Residential location choice: models and applications**. Springer Science & Business Media.

West, G. (2017). **Scale: The universal laws of life, growth, and death in organisms, cities, and companies**. Penguin.

West, G., Brown, J., y Enquist, B. (2001, 11). A general model for ontogenic growth. **Nature**, 413, 628-31. doi: 10.1038/35098076

West, G. B. (1999). The origin of universal scaling laws in biology. **Physica A: Statistical Mechanics and its Applications**, 263 (1), 104-113. Descargado de https://www.sciencedirect.com/science/article/pii/S0378437198006396 (Proceedings of the 20th IUPAP International Conference on Statistical Physics) doi: https://doi.org/10.1016/S0378-4371(98)00639-6

West, G. B., Brown, J. H., y Enquist, B. J. (1999). The fourth dimension of life: Fractal geometry and allometric scaling of organisms. **Science**, 284 (5420), 1677-1679. Descargado de https://www.science.org/doi/abs/10.1126/science.284.5420.1677 doi: 10.1126/science.284.5420.1677